High-Temperature Thermodynamic and Transport Properties of Planetary CO_2 — N_2 Atmospheres

G. N. Freeman* and C. C. Oliver†
Purdue University, Lafayette, Ind.

A general method for computing equilibrium thermodynamic and transport properties of reacting planetary atmospheres is summarized. Equilibrium composition and derivatives are established from first principles, permitting calculation of total specific heat, thermal conductivity, and Prandtl number. Results are presented for two CO_2 — N_2 atmospheres in dissociative equilibrium over a range of temperature and pressure bracketing expected conditions during Martian or Venusian entry.

I. Introduction

In hypersonic flows chemical reactions profoundly affect the compressibility and temperature of the fluid and, therefore, the thermodynamic and radiative coupling in the flow. Transport processes in the flowfield exhibit a similar dependence on the chemical composition. Under conditions of local equilibrium, the thermodynamic and transport properties can be correlated in terms of two independent thermodynamic variables for a given elemental composition. The resulting simplification in obtaining flowfield solutions is enormous compared to the general nonequilibrium case because solution of the individual species conservation equations is not required. A general method which possesses the accuracy and speed required in engineering calculations is outlined here for computing the properties. Results are presented for CO_2 — N_2 equilibrium atmospheres.

The validity of the equilibrium assumption depends upon the time necessary for the system to come to a steady state with respect to a given perturbation. Since the rates of internal energy exchange and chemical reaction depend upon collision frequency, the rapid attainment of equilibrium is favored at lower altitudes and higher flight velocities. Because trajectory times are proportional to the scale of the flowfield, equilibrium is also favored for larger vehicles. The mapping of the trajectory regions over which the equilibrium assumption is applicable requires knowledge of the pertinent nonequilibrium rates. A comparison of equilibrium and nonequilibrium flows has been made[1] for blunt entry vehicles in CO_2 — N_2 atmospheres and is to be reported in a subsequent paper.

An extensive literature exists on the calculation of high-temperature thermodynamic and transport properties of equilibrium gas mixtures. The purpose here was to consolidate this information in a consistent manner and to present results using recent collision cross-section data for postulated Martian and Venusian atmospheres.

II. Analysis

Reactive Properties

All the thermodynamic properties of a pure gas can be calculated from its partition function. For example, the Gibbs free energy depends upon the partition function itself; the internal energy, enthalpy, and entropy upon the first derivative; and the specific heats, various isentropic functions, and the velocity of sound upon the second derivative. Browne[2–5] performed such calculations for the constituents of reacting planetary atmospheres and his results were used here.

One of several classical methods (such as the minimization of the mixture free energy) is commonly employed to compute the equilibrium properties of the mixture in terms of the thermodynamic functions of the individual species. Closed form solutions[6] are practical only for relatively simple chemical systems. For more complex systems an iterative solution[7,8] is required. The number of simultaneous nonlinear algebraic equations to be solved is equal to the number of chemical elements in the mixture.

Consideration is given to a closed system in which the masses of the components are changed by chemical reactions within the system. For a fixed temperature and pressure at equilibrium, the variation of the free energy of a mixture of ideal gases is given by

$$\left.\frac{\delta G}{RT}\right|_{T,P} = \sum_{i=1}^{\nu}\left[\ln(PX_i) + \frac{\mu_i^0}{RT}\right]\delta N_i = 0 \qquad (1)$$

where G = Gibbs free energy of mixture, N_i = number of moles of species i, P = absolute pressure, R = universal gas constant, T = absolute temperature, X_i = mole fraction of species i, μ_i^0 = chemical potential of species i at one atmosphere, and ν = number of chemical species in mixture.

Not all the δN_i are independent, but are subject to the constraints of elemental mass and charge conservation as follows:

$$\tilde{N}_j = \sum_{i=1}^{\nu}\alpha_{ij}N_i \quad [j = 1,2,\ldots\mu] \qquad (2)$$

where $\tilde{N}j$ = number of moles of element j (or net charge) existing in all forms, α_{ij} = number of atoms of element j (or net charge) per molecule i, and μ = number of chemical elements in mixture.

The summations (1) and (2) are separated for convenience into sums over the free atoms and electrons ($1 \leq j \leq \mu$) and combined species ($\mu + 1 \leq i \leq \nu$). Noting that $\delta\tilde{N}j = 0$, Eq. (2) is differentiated and substituted into Eq. (1) with the result,

$$\sum_{i=\mu+1}^{\nu}\left\{\left[\ln(PX_i) + \frac{\mu_i^0}{RT}\right] - \sum_{j=1}^{\mu}\alpha_{ij}\left[\ln(PX_j) + \frac{\mu_j^0}{RT}\right]\right\}\delta N_i = 0 \qquad (3)$$

The δN_i for the combined species are independent; hence, the bracketed quantity is zero for all i. In terms of the mole frac-

Received October 6, 1969; revision received March 9, 1970.
* Research Assistant. Associate Member AIAA.
† Associate Professor, Department of Mechanical Engineering; presently Professor, Department of Mechanical Engineering, University of Florida. Member AIAA.

tion X_i there results

$$\ln X_i = \ln K_i(T) + (\beta_i - 1)\ln P + \sum_{j=1}^{\mu} \alpha_{ij} \ln X_j \quad [i = (\mu + 1),\ldots,\nu] \quad (4)$$

where

$$\ln K_i(T) = -\frac{\mu_i^0}{RT} + \sum_{j=1}^{\mu} \alpha_{ij} \frac{\mu_j^0}{RT} \quad (5)$$

$$\beta_i = \sum_{j=1}^{\mu} \alpha_{ij} \quad (6)$$

$K_i(T)$ is the equilibrium constant for formation of the $(\nu - \mu)$ molecules and ions from the μ atoms and electrons; β_i is the number of atoms and charges j in the molecule or ion i. The $(\nu - \mu)$ mass action Eq. (4) must be augmented by μ mass balance equations in order that the system for the unknown X_i be determinate. A suitable relation may be derived by normalizing Eq. (2) by its sum over the elements $1 \leq j \leq \mu$. Thus,

$$\tilde{X}_j = \left[\sum_{i=1}^{\nu} \alpha_{ij} X_i\right]\left[\sum_{i=1}^{\nu} \beta_i X_i\right]^{-1} \quad [j = 1,\ldots,\mu] \quad (7)$$

where $\tilde{X}_j$ = particle fraction of element j existing in all forms =

$$\tilde{N}_j \Big/ \sum_{m=1}^{\mu} \tilde{N}_m$$

The summations in Eq. (7) are separated, as before, into sums over combined and uncombined species. Solving for the uncombined mole fraction X_j yields the following result:

$$X_j = \tilde{X}_j + \sum_{i=\mu+1}^{\nu} [(\beta_i - 1)\tilde{X}_j - \alpha_{ij}]X_i \quad [j = 1,\ldots,\mu] \quad (8)$$

Forming the exponential of Eq. (4) and substituting the result into Eq. (8) yields the following μ dimensional nonlinear system

$$X_j = \tilde{X}_j + \sum_{i=\mu+1}^{\nu} [(\beta_i - 1)\tilde{X}_j - \alpha_{ij}]K_i(T)P^{(\beta i - 1)} \times \prod_{m=1}^{\mu} X_m^{\alpha_{im}} \quad [j = 1,\ldots,\mu] \quad (9)$$

Equation (9) is readily solved by Newton-Raphson iteration with expansion in terms of the $\ln X_j$. Convergence is most rapid where the atomic and electronic mole fractions X_j are large; convergence at low temperatures is best achieved by stepping downwards in temperature, using the previous converged values for X_j as the initial guesses at the subsequent step. The molecular and ionic mole fractions X_i then follow directly from Eq. (4).

The equilibrium composition is sufficient to determine all thermodynamic and transport properties of interest except the equilibrium mass specific heat C_p and total thermal conductivity λ. These quantities are defined only at local equilibrium in regions of uniform pressure and elemental composition and include contributions due to concentration gradients,[9] as follows:

$$C_p = \tilde{C}_p + \left(\frac{z}{M_0}\right) \sum_{i=1}^{\nu} X_i(h_i - hM_i)\left[\frac{\partial \ln X_i}{\partial T}\right]_{P,\nabla\tilde{X}_j=0} \quad [j = 1,\ldots,\mu] \quad (10)$$

$$\lambda = \bar{\lambda} - \frac{P}{RT} \sum_{i=1}^{\nu} h_i \left[\frac{X_i \mathbf{V}_i}{\nabla T}\right]_{P,\tilde{\mathbf{V}}_j=0} \quad [j = 1,\ldots,\mu] \quad (11)$$

where $\tilde{C}_p$ = frozen mass specific heat of mixture =

$$\left(\frac{z}{M_0}\right) \sum_{i=0}^{\nu} X_i C_{pi}$$

C_{pi} = molar specific heat of species i, h_i = molar enthalpy of species i,

$$h = \text{mass enthalpy of mixture} = \left(\frac{z}{M_0}\right) \sum_{i=1}^{\nu} X_i h_i$$

M_i = molecular weight of species i, M_0 = molecular weight of undissociated mixture, $\mathbf{V}_i$ = mass diffusion velocity of species i, $\tilde{\mathbf{V}}_j$ = mass diffusion velocity of element j =

$$\left[\sum_{i=1}^{\nu} \alpha_{ij} X_i \mathbf{V}_i\right]\left[\sum_{i=1}^{\nu} \alpha_{ij} X_i\right]^{-1}$$

$$Z = \text{compressibility} = M_0 \Big/ \sum_{i=1}^{\nu} X_i M_i$$

∇ = gradient, and $\bar{\lambda}$ = frozen thermal conductivity of mixture. The summations in Eqs. (10) and (11) are more conventionally written in mass rather than molar units.

The ratios $X_i \mathbf{V}_i / \nabla T$ are related to the concentration gradients in an equilibrium flow of uniform pressure and elemental composition through the multicomponent diffusion relation as follows:

$$\frac{1}{X_i}\left[\frac{\nabla X_i}{\nabla T}\right] = \left[\frac{\partial \ln X_i}{\partial T}\right] = \sum_{k=1}^{\nu} \frac{X_k}{\mathfrak{D}_{ik}}\left[\frac{\mathbf{V}_k}{\nabla T} - \frac{\mathbf{V}_i}{\nabla T}\right] \quad [i = 1,\ldots,\nu] \quad (12)$$

where $\mathfrak{D}_{ik}$ = binary diffusion coefficient.

For the simultaneous diffusion of more than two species, the diffusion velocity of a species is not simply proportional to its concentration gradient. Thus, the partial derivatives (12) required for Eq. (11) are not equivalent to those in Eq. (10). In both cases $(\nu - \mu)$ relations are provided by differentiating the mass action Eq. (4) with respect to temperature. The additional relations are provided in the case of Eq. (10) by differentiating the mass balance relation (8), and in the case of Eq. (11) by combining the defining relation for $\tilde{\mathbf{V}}_j$ (equal zero) with Eq. (12). After considerable algebraic manipulation, the $[\partial \ln X_i / \partial T]_{P,\nabla\tilde{X}_j=0}$ are given by the μ-dimensional linear system[1] as follows:

$$\sum_{k=1}^{\mu} a_{jk}[\partial \ln X_k / \partial T]_{P,\nabla\tilde{X}_n=0} = b_j \quad [j,n = 1,\ldots,\mu] \quad (13)$$

where

$$a_{jk} = -\sum_{i=\mu+1}^{\nu} [(\beta_i - 1)\tilde{X}_j - \alpha_{ij}]\alpha_{ik}X_i \quad [j \neq k]$$

$$a_{jj} = a_{jk}|_{k=j} + X_j$$

$$b_j = \sum_{i=\mu+1}^{\nu} [(\beta_i - 1)\tilde{X}_j - \alpha_{ij}] \times \left[h_i/RT^2 - \sum_{k=1}^{\mu} \alpha_{ik}h_k/RT^2\right] X_i$$

The remaining $(\nu - \mu)$ derivatives follow directly from the derivative of Eq. (4).

The $[X_i \mathbf{V}_i / \nabla T]_{P,\tilde{\mathbf{V}}_j=0}$ are determined from the $(\nu - \mu)$ dimensional linear system[1] as follows:

$$\sum_{m=\mu+1}^{\nu} a_{im}\left[\frac{X_m \mathbf{V}_m}{\nabla T}\right]_{P,\tilde{\mathbf{V}}_j=0} = b_i \quad [j = 1,\ldots,\mu;\ i = \mu + 1,\ldots,\nu] \quad (14)$$

where

$$a_{im} = \frac{1}{\mathfrak{D}_{im}} + \sum_{j=1}^{\mu}\left[-\frac{\alpha_{mj}}{\mathfrak{D}_{ij}} + a_{ij}\left(-\frac{1}{\mathfrak{D}_{mj}} + \sum_{n=1}^{\mu}\frac{\alpha_{mn}}{\mathfrak{D}_{jn}} - \frac{\alpha_{mj}}{X_j}\sum_{q=1}^{\nu}\frac{X_q}{\mathfrak{D}_{jq}}\right)\right] \quad (i \neq m)$$

$$\alpha_{ii} = \alpha_{im}|_{m=i} - \frac{1}{X_i}\sum_{m=1}^{\nu}\frac{X_m}{\mathfrak{D}_{im}}$$

$$b_i = h_i/RT^2 - \sum_{j=1}^{\mu}\alpha_{ij}h_j/RT^2$$

The remaining μ diffusion terms follow directly from the defining relation for $\tilde{\mathbf{V}}_j = 0$:

$$\left[\frac{X_j\mathbf{V}_j}{\nabla T}\right]_{P,\tilde{\mathbf{V}}_n=0} = -\sum_{i=\mu+1}^{\nu}\alpha_{ij}\left[\frac{X_i\mathbf{V}_i}{\nabla T}\right]_{P,\tilde{\mathbf{V}}_n=0} \qquad [j,n = 1,\ldots,\mu] \tag{15}$$

Note that when applied to charged species, Eq. (15) amounts to the requirement of ambipolar diffusion.

Kinetic Properties

Until ionization becomes appreciable, the first order Chapman-Enskog formulas yield predictions that are consistent in accuracy with the collision cross sections.[10] In the following formulas the quantities A_{ij}^* and B_{ij}^* are defined in the usual manner following Hirshfelder et al[11]:

$$A_{ij}^* = \bar{\Omega}_{ij}^{(2,2)}/\bar{\Omega}_{ij}^{(1,1)} \tag{16}$$

$$B_{ij}^* = [5\bar{\Omega}_{ij}^{(1,2)} - 4\bar{\Omega}_{ij}^{(1,3)}]/\bar{\Omega}_{ij}^{(1,1)} \tag{17}$$

where the collision integrals $\bar{\Omega}_{ij}^{(l,s)}$ are equivalent to $\sigma_{ij}^2\Omega_{ij}^{(l,s)*}$ in Hirschfelder's notation. The formulas are equivalent to those of Ref. 11 but differ in form. Here the subscripts i,j are not to be associated with combined and uncombined species as above.

Viscosity

Let the coefficient matrix E_{ij} be defined as

$$E_{ij} = 2X_j/(M_i + M_j)P\mathfrak{D}_{ij} \quad [i,j = 1,2,\ldots,\nu]$$

Further define the coefficient matrix H_{ij} as

$$H_{ij} = -E_{ij}(1 - 3A_{ij}^*/5) \quad [i \neq j]$$

$$H_{ii} = H_{ij}|_{j=i} + \sum_{j=1}^{\nu}E_{ij}\left(1 + \frac{3M_j}{5M_i}A_{ij}^*\right)$$

The viscosity is then given by

$$\eta = \frac{1}{RT}\sum_{i=1}^{\nu}c_iX_i \tag{18}$$

where c_i is the solution of the linear system

$$\sum_{j=1}^{\nu}H_{ij}C_j = 1$$

Frozen thermal conductivity

Let the coefficient matrix F_{ij} be defined as

$$F_{ij} = 2M_iM_jE_{ij}/(M_i + M_j) \quad [i,j = 1,2,\ldots,\nu]$$

Further define the coefficient matrix L_{ij} as

$$L_{ij} = F_{ij}[\tfrac{5}{16}\tfrac{5}{6} - 3B_{ij}^*/4 - A_{ij}^*] \quad [i \neq j]$$

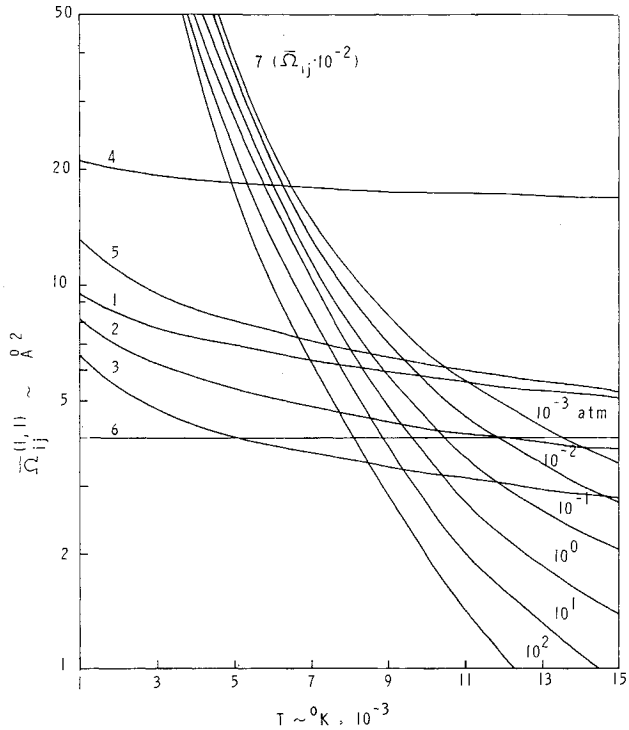

Fig. 1 Collision integral $\bar{\Omega}_{ij}^{(1,1)}$.

$$L_{ii} = L_{ij}|_{j=i} - \sum_{j=1}^{\nu}F_{ij}\left[\frac{15M_i}{8M_j} + \left(\frac{25}{16} - \frac{3}{4}B_{ij}^*\right)\frac{M_j}{M_i} + A_{ij}^*\right]$$

The frozen thermal conductivity is then given by

$$\bar{\lambda} = -\left(\frac{25}{4T}\right)\sum_{i=1}^{\nu}d_iX_i + \lambda^E \tag{19}$$

where d_i is the solution of the linear system

$$\sum_{j=1}^{\nu}L_{ij}d_j = 1$$

and where

$$\lambda^E = \left(\frac{1}{T}\right)\sum_{i=1}^{\nu}X_i\left[\frac{C_{pi}}{R} - \frac{5}{2}\right]\left[\sum_{j=1}^{\nu}\frac{X_j}{P\mathfrak{D}_{ij}}\right]^{-1} \tag{20}$$

Equation (20) is the modified Eucken correction to account for energy storage in excited molecular states.

The pressure-independent product $P\mathfrak{D}_{ij}$ occurring in these relations is related simply to the collision integral $\bar{\Omega}_{ij}^{(1,1)}$ as follows:

$$P\mathfrak{D}_{ij} = (\tfrac{3}{8}[(RT)^3(M_i + M_j)/2\pi M_iM_j]^{1/2}/\bar{\Omega}_{ij}^{(1,1)} \tag{21}$$

The collision data $\bar{\Omega}_{ij}^{(1,1)}$, A_{ij}^*, and B_{ij}^* that appear in Figs. 1–3 include the effects of multiple-interaction potentials,[12] resonant charge exchange,[12] and Debye shielding.[13] Characteristic interactions are designated by a numerical index (1–7) and are identified in Table 1. The identity of the participants beyond the classifications in the table is not required to obtain results consistent in accuracy with the collision integrals.

The neutral particle interactions 1–3 were taken as averages of the corresponding values from Ref. 14. Interaction 4 between an ion and its parent atom was taken from Refs. 15 ($\bar{\Omega}_{ij}^{(2,2)}$) and 16 ($\bar{\Omega}_{ij}^{(1,1)}$). The nonresonant integral $\bar{\Omega}_{ij}^{(2,2)}$ for interaction 4 was assumed to describe adequately the cor-

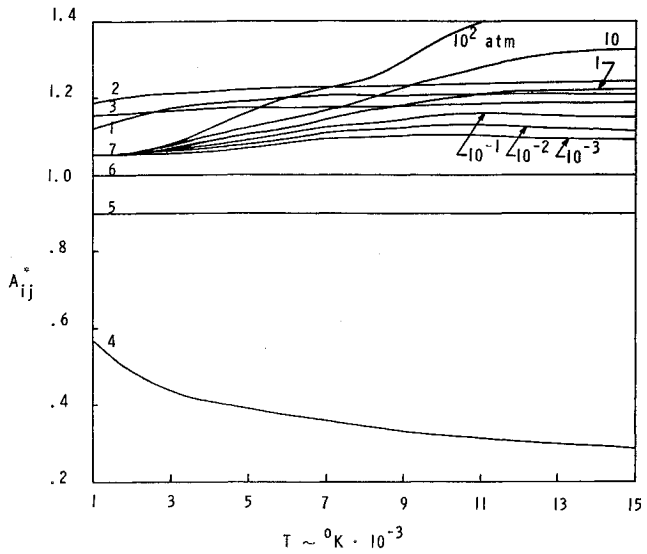

Fig. 2 Ratio of collision integrals A_{ij}*; Eq. (16).

responding integral for interaction 5 between dissimilar atom-ion pairs. The $\bar{\Omega}_{ij}^{(1,1)}$ integral for this interaction has not been studied in detail; it was estimated here using the relation $\bar{\Omega}_{ij}^{(1,1)} = \bar{\Omega}_{ij}^{(2,2)}/A_{ij}^*$ with $A_{ij}^* = 0.9$. This value was obtained by comparing the results of Ref. 17 ($\bar{\Omega}_{ij}^{(2,2)}$) with those of Ref. 18 ($\bar{\Omega}_{ij}^{(1,1)}$), both of which were based on a crude Morse-plus-polarization ground state potential. No reliable estimates were available for interaction 6 between an electron and a neutral particle. Various approximations[15,17–19] have been attempted and are in poor agreement. The value $\bar{\Omega}_{ij}^{(1,1)} = \bar{\Omega}_{ij}^{(2,2)} = 4.0$ was chosen as representative of these estimates. For lack of better information, the quantity B_{ij}^*, which is always of order unity, was set equal to 1 for interactions 4–6.

Interaction 7 between charged particles was investigated in Ref. 13 for a fully ionized gas. The collision was described by a shielded Coulomb potential where the shielding accounts for long-range multiple particle interactions arising from the charge background. The resulting collision integrals were applied here to the region of partial ionization. Because the concept of a binary collision does not strictly apply, the strength of the interaction depends upon the proximity of adjacent charges. From Fig. 1 it is observed that the interaction is strengthened as the pressure (and the number density of charged particles) decreases.

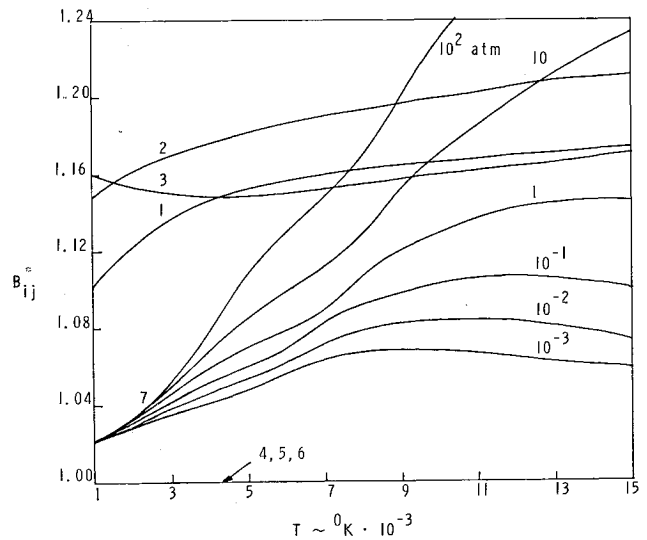

Fig. 3 Ratio of collision integrals B_{ij}*; Eq. (17).

Table 1 Characteristic interactions

Index	Type of Interaction
1	Molecule-molecule (molecule-molecular ion)
2	Atom-molecule (molecule-atomic ion, atom-molecular ion)
3	Atom-atom
4	Atom-similar atomic ion
5	Atom-dissimilar atomic ion
6	Electron-atom (electron-molecule)
7	Charged-charged

III. Results

Calculations were performed for equilibrium conditions bracketing the range expected during Martian or Venusian entry. Two atmospheres were considered: 50–50 and 90–10 $CO_2 - N_2$ by volume. Dissociation products included those which were expected to make appreciable contributions to the thermodynamic or radiative properties of the gas: CO_2, N_2, C_2, O_2, CN, CO, NO, C, N, O, C^+, N^+, O^+, NO^+, e^-. The results reflect the dominant chemical behavior of the reacting gas. Properties of the undissociated mixture are shown for comparison; these represent the infinite pressure (no reaction) limit of the equilibrium mixture.

Thermodynamic Properties

The predominant types of reaction are indicated in Fig. 4 and are seen to be reflected in rather abrupt increases in the compressibility. The values of compressibility are always higher for the 90–10 mixture by an amount determined almost entirely by the relative influence of the CO_2 dissociation reaction (i.e., by the cold mixture CO_2 mole fraction).

The mass enthalpy for a given mixture (Fig. 5) exhibits a behavior similar to that of the compressibility. Two complimentary effects are at work: 1) the chemical enthalpy of the dominant equilibrium species increases with temperature, causing an increase in the enthalpy per mole of mixture; and 2) the molecular weight decreases with increasing temperature so that the mass enthalpy rises more rapidly than the molar enthalpy. Differences between the two dissociating mixtures reflect the relative CO_2/N_2 concentrations in the cold gas. By conservation of energy the enthalpy of the fully dissociated mixture is roughly independent of the cold composition; the independence remains through ionization because the ionization energies of C, N, and O are comparable.

The frozen mass specific heat (Fig. 6) exhibits the same over-all behavior as the enthalpy, except for near constancy through the first dissociation (CO_2) and a decrease at constant temperature as the degree of dissociation increases below

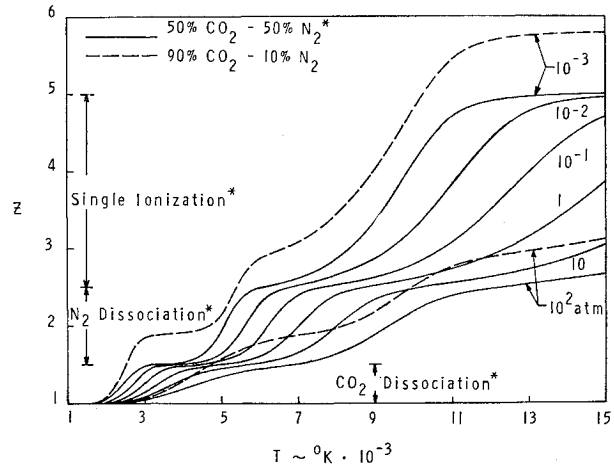

Fig. 4 Compressibility.

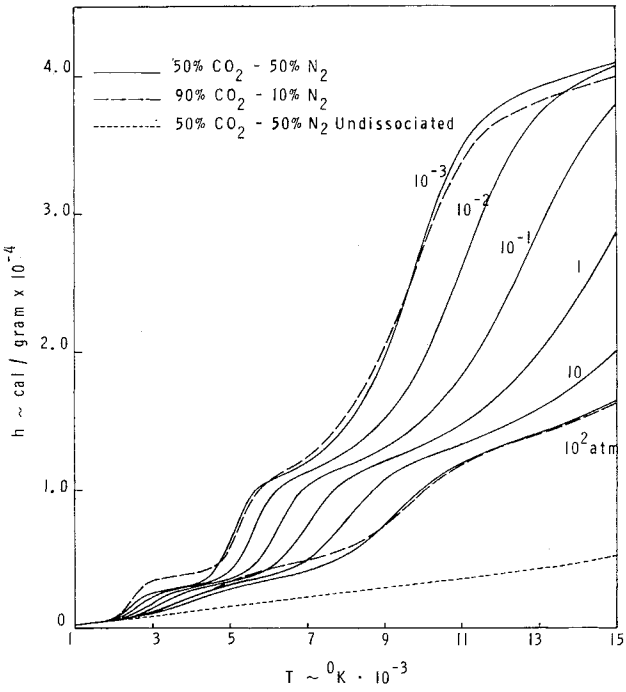

Fig. 5 Specific enthalpy.

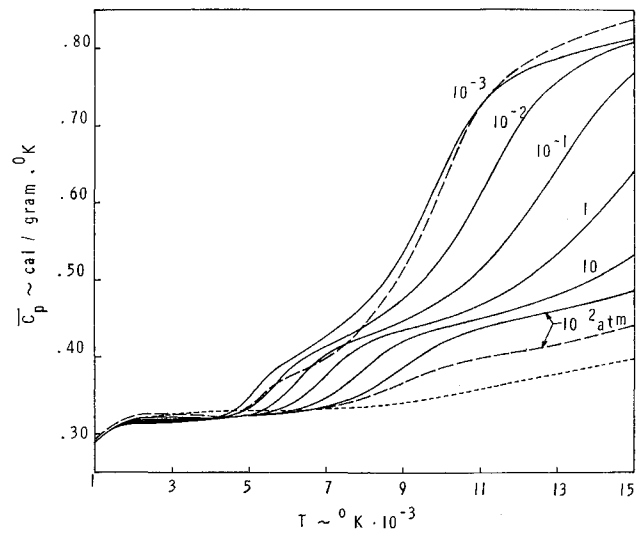

Fig. 6 Frozen specific heat (same legend as Fig. 5).

4000°K. These differences arise because the two effects which are complimentary for the enthalpy are opposed for the specific heat. Namely, the specific heat of the dominant equilibrium species decreases as the temperature increases, causing a decrease in the molar specific heat of the mixture. This effect dominates slightly the decreasing molecular weight below 4000°K; above 4000°K the effect of decreasing molecular weight dominates until at the higher temperatures the curves for mass specific heat closely resemble those for mass enthalpy. Comparing the two mixtures, it is seen that the specific heat for the 90–10 mixture is generally higher below 4000°K and lower above, until ionization becomes appreciable. This is a reflection of the higher specific heat of CO_2 compared to N_2 and a lower specific heat of the dissociation products of CO_2 compared to those of N_2.

The equilibrium mass specific heat is shown in Fig. 7. The energy absorbed and released by chemical reaction as transmitted to the specific heat through the temperature derivatives of composition is seen to dominate the energy carried in the translational and internal modes at all but the lowest temperatures. At the highest pressure considered (100 atm) the curve for equilibrium specific heat begins to resemble its frozen counterpart, but it remains quantitatively higher. The decreasing height and rightward shift of the peaks with increasing pressure is a result of the decreasing extent of reaction and the greater energy required to produce reaction at the higher pressures. By comparison with Fig. 4, it is seen that the first peaks are due to the CO_2 dissociation, the second to the N_2 dissociation, and the third to single ionization. The height of the first peak therefore increases with the relative CO_2 concentration whereas that of the second decreases.

Transport Properties

For the interpretation of trends, it is useful to visualize a representative collision cross section for the equilibrium mixture as a whole. The properties of the mixture may then be interpreted in terms of the familiar concepts and simple kinetic formulae for a pure gas. The cross section may be taken to be the population-weighted average of the participating collision integrals at a given temperature and pressure. In the neighborhood of 1000°K the cross section has the value corresponding to molecular interactions. It decreases somewhat in the intermediate dissociation region due to the influence of the smaller atomic collision integrals. An abrupt increase accompanies the onset of ionization as the Coulombic interactions become more important.

The required pure gas relations follow from Eqs. (18) and (19) with $\nu = 1$:

$$\eta = 5M_0P\mathfrak{D}/6RTA^* \tag{22}$$

$$\bar{\lambda} = [25/8A^* + (C_p/R - 5/2)]P\mathfrak{D}/T \tag{23}$$

where, from Eq. (21)

$$P\mathfrak{D} = 3[(RT)^3/\pi M_0]^{1/2}/8\bar{\Omega}^{(1,1)} \tag{24}$$

It is apparent that the transport coefficients of a pure gas or nonreacting mixture increase with temperature (the collision integrals decrease) and are independent of pressure. Differences in the presence of chemical reaction are due to changes in molecular weight or in the "average" collision cross section. Neglecting changes in molecular weight, the viscosity and frozen thermal conductivity can be expected first to increase due to dissociation, then to decrease due to ionization. The variation in viscosity compared to conductivity should be smaller during dissociation and larger during ionization due to changes in molecular weight.

The viscosity curves appear in Fig. 8. Comparison with the equilibrium composition confirms that the maximum dis-

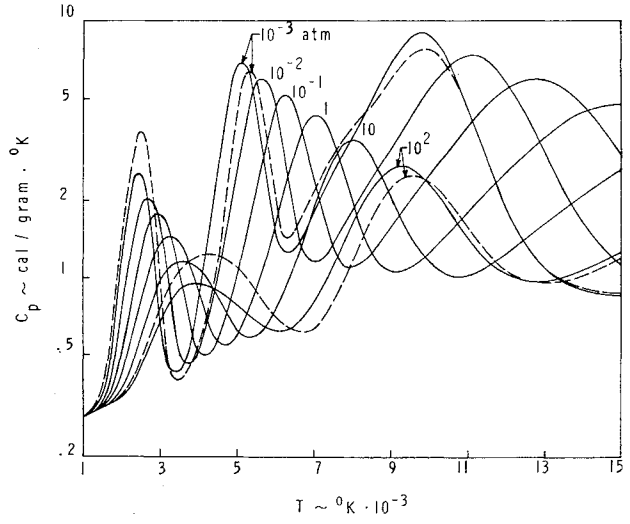

Fig. 7 Equilibrium specific heat (same legend as Fig. 4).

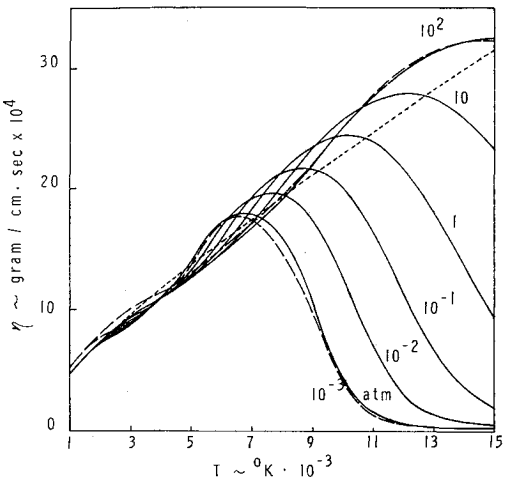

Fig. 8 Viscosity (same legend as Fig. 5).

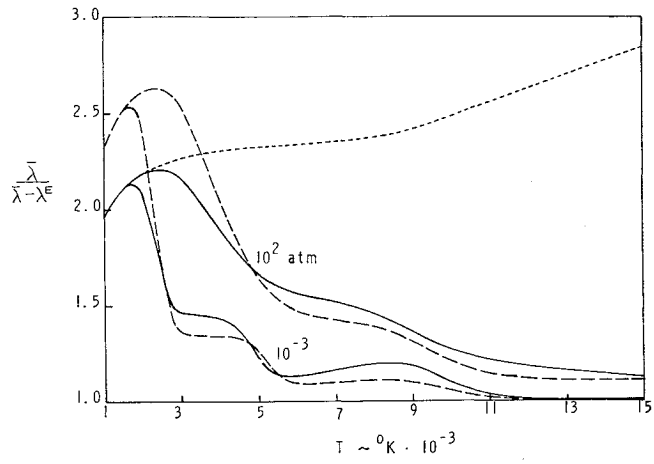

Fig. 10 Effect of internal energy on frozen thermal conductivity (same legend as Fig. 5).

tance to which an equilibrium curve rises above the frozen curve occurs at the temperature corresponding to peak atom concentration at each pressure considered. The abrupt drop at higher temperatures follows from the large collision integrals of the increasingly important charged-charged interactions. The final significant characteristic is the dominance of the molecular weight influence at the relatively low temperatures corresponding to CO_2 dissociation. Dissociation is more rapid at the lower pressures, causing a greater depression of the lower pressure viscosity curves. The inversion below 4000°K reflects the influence of competing effects in the same manner as observed for the frozen specific heat.

The trends observed in Fig. 9 for the frozen thermal conductivity are generally similar to those for viscosity. The absence of a significant depression in the CO_2 dissociation region is due to the fact that a decreasing molecular weight tends to increase the thermal conductivity, in contrast to its effect on viscosity. Another factor is the effect of internal energy storage which has been included in Fig. 9.

The contribution of internal energy states to the thermal conductivity is shown in Fig. 10. The ratio of conductivity including internal energy effects is normalized with respect to the conductivity neglecting internal energy. It is seen that at low temperatures the internal energy modes contribute an amount nearly equal to that due to translational energy exchange; the effect increases with CO_2 enrichment because of the greater capacity for internal energy storage. As the translational energy increases, the relative importance of the internal mode decreases.

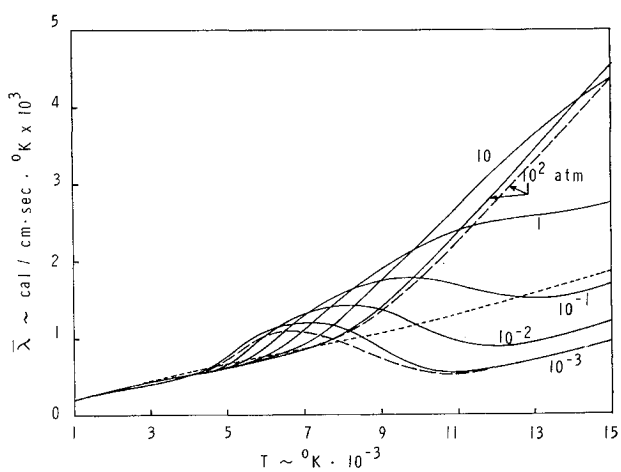

Fig. 9 Frozen thermal conductivity (same legend as Fig. 5).

Over the temperature range investigated, the absolute magnitude of the internal energy contribution remained at about the same order. This is due to two competing effects: 1) $(C_{pi} - 5R/2)$ increases with temperature, causing a corresponding increase in the internal energy stored per particle; and 2) the equilibrium fraction of particles capable of significant internal energy storage (i.e., in the vibrational mode) decreases with increasing temperature. Note from Fig. 10 that the internal energy correction extends to higher temperatures at higher pressures due to the smaller degree of dissociation which has occurred.

The total thermal conductivity including translational, internal, and chemical contributions is shown in Fig. 11. Comparison with Fig. 7 for the equilibrium specific heat indicates that both functions exhibit local maxima at about the same temperatures. However, the ionization peaks in Fig. 11 are less pronounced than in Fig. 7 because the large Coulombic collision integrals impede the diffusion process at high temperatures. At very low temperatures, on the other hand, dissociation is slight, and the thermal conductivity increment due to reaction becomes negligible.

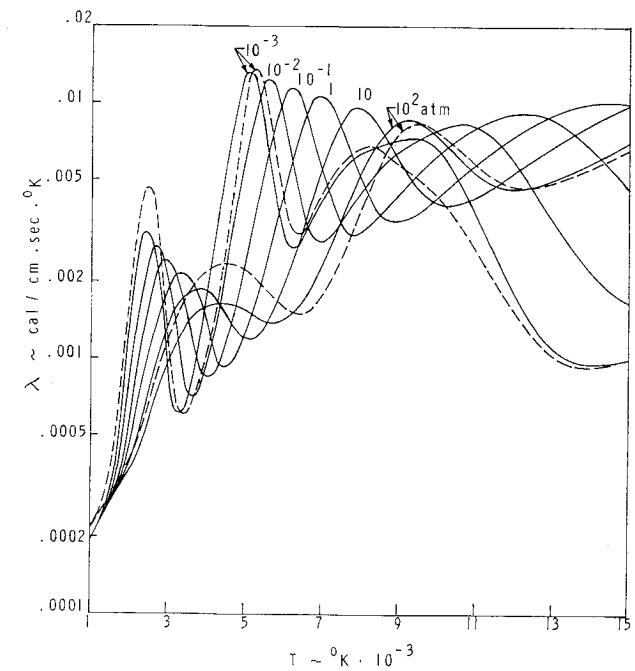

Fig. 11 Equilibrium thermal conductivity (same legend as Fig. 4).

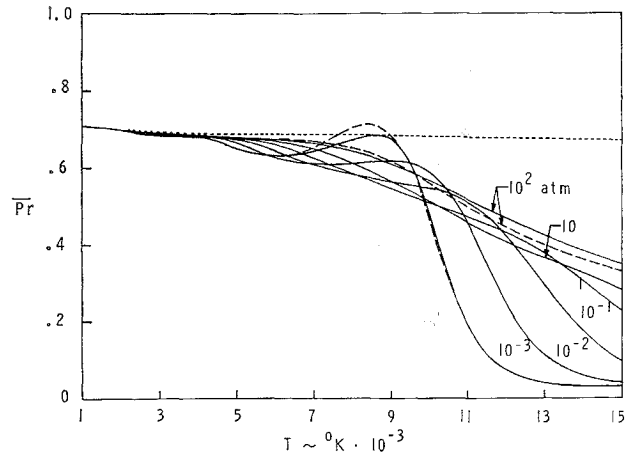

Fig. 12 Frozen Prandtl number (same legend as Fig. 5).

The frozen Prandtl number $\mu\bar{C}_p/\bar{\lambda}$ appearing in Fig. 12 combines the results of Figs. 6, 8, and 9; the equilibrium Prandtl number $\mu C_p/\lambda$ appearing in Fig. 13 combines the results of Figs. 7, 8, and 11. The peaks occurring in equilibrium specific heat and thermal conductivity do not necessarily cancel in forming the ratio because the peaks may be slightly displaced on a temperature scale.[19] Thus, the equilibrium Prandtl number reflects the oscillatory character of its components.

In conclusion, it is observed that the equilibrium reactive properties C_p and λ are extremely temperature-sensitive and that these quantities usually dominate their frozen counterparts $\bar{C}_p$ and $\bar{\lambda}$. A slight phase shift in the calculated thermal conductivity peaks significantly affects the resulting Prandtl number. Thus, failure of the chemistry to follow the rapid variations implied by local equilibrium could cause the present predictions to be in serious error. In spite of these difficulties the equilibrium formalism has been successful in solutions of reacting flowfields over a wide range of conditions of practical interest and should be applicable to Venusian and low altitude Martian entry.

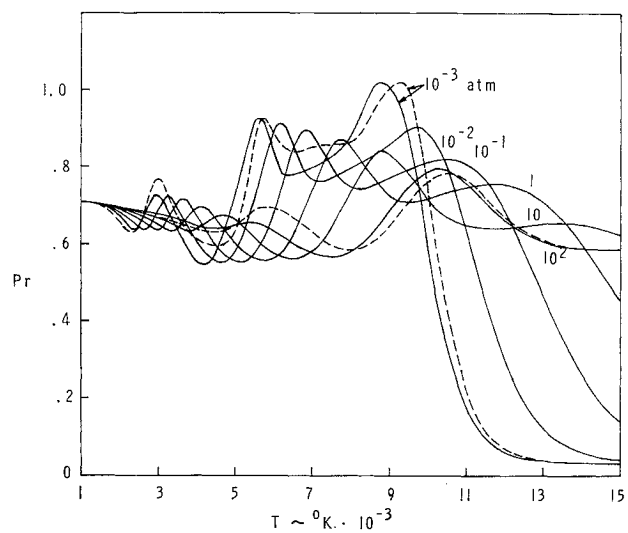

Fig. 13 Equilibrium Prandtl number (same legend as Fig. 4).

References

[1] Freeman, G. N., *The Thermochemistry of Nonequilibrium, Viscous, Radiating, Blunt Body Shock Layers in CO_2-N_2 Atmospheres*, Ph.D. thesis, Jan. 1969, Purdue Univ.

[2] Browne, W. G., "Thermodynamic Properties of Some Atoms and Atomic Ions," Engineering Physics Technical Memo 2, General Electric Missiles and Space Systems Div., Valley Forge, Pa.

[3] Browne, W. G., "Thermodynamic Properties of Some Diatoms and Diatomic Ions at High Temperatures," Advanced Aerospace Physics Technical Memo 8, May 1962, General Electric Missiles and Space Systems Div., Valley Forge, Pa.

[4] Browne, W. G., "Thermodynamic Properties of Some Diatomic and Linear Polyatomic Molecules," Engineering Physics Technical Memo 3, General Electric Missiles and Space Systems Div., Valley Forge, Pa.

[5] Browne, W. G., "Thermodynamic Properties of the Species CN, C_2, C_3, C_2N_2, and C^-," Advanced Aerospace Physics Technical Memo 9, May 1962, General Electric Missiles and Space Systems Div., Valley Forge, Pa.

[6] Erickson, W. D., Kemper, J. T., and Allison, D. O., "A Method for Computing Chemical Equilibrium Compositions of Reacting Gas Mixtures by Reduction to a Single Iteration Equation," TN D-3488, Aug. 1966, NASA.

[7] Gordon, S., Zeleznik, F. J., and Huff, V. N., "A General Method for Automatic Computation of Equilibrium Compositions and Theoretical Rocket Performance of Propellants," TN D-132, Oct. 1959, NASA.

[8] Peng, T. C., Doane, P. M., and Fivel, H. J., "Model Optimization of Equilibrium Air Plasmas from 10^{-4}-10^3 Atm and 1000 to 10000°K," Rept. G996, March 1969, McDonnell Research Lab., St. Louis, Mo.

[9] Butler, J. N. and Brokaw, R. S., "Thermal Conductivity of Gas Mixtures in Chemical Equilibrium," *Journal of Chemical Physics*, Vol. 26, No. 6, June 1957, pp. 1636–1643.

[10] Ahtye, W. F., "A Critical Evaluation of Methods for Calculating Transport Coefficients of Partially and Fully Ionized Gases," TN D-2611, Jan. 1965, NASA.

[11] Hirschfelder, J. O., Curtiss, C. F., and Bird, R. B., *Molecular Theory of Gases and Liquids*, Wiley, New York, March 1964, pp. 528, 531–538, 1196–1197.

[12] Mason, E. A., Vanderslice, J. T., Yos, J. M., "Transport Properties of High-Temperature Multicomponent Gas Mixtures," *The Physics of Fluids*, Vol. 2, No. 6, Nov.–Dec. 1959, pp. 688–694.

[13] Liboff, R. L., "Transport Coefficients Determined Using the Shielded Coulomb Potential," *The Physics of Fluids*, Vol. 2, No. 1, Jan.-Feb. 1959, pp. 40–46.

[14] Yun, K. S. and Mason, E. A., "Collision Integrals for the Transport Properties of Dissociating Air at High Temperatures," *The Physics of Fluids*, Vol. 5, No. 4, April 1962, pp. 380–386.

[15] Sherman, M. P., "Transport Properties of Partially Ionized Nitrogen I. The Collision Integrals," Rept. R65SD4, July 1965, General Electric Missiles and Space Systems Div., Valley Forge, Pa.

[16] Knof, H., Mason, E. A., and Vanderslice, J. T., "Interaction Energies, Charge Exchange Cross Sections, and Diffusion Cross Sections for N+-N and O+-O Collisions," *Journal of Chemical Physics*, Vol. 40, No. 12, June 1964, pp. 3548–3553.

[17] Yos, J. M., "Transport Properties of Nitrogen, Hydrogen, Oxygen, and Air to 30000°K," RAD-TM-63-7, 1963, Avco Corp., Wilmington, Mass.; also, ASD-TDR-62-729, Pt. II, Vol. 2, 1963, U.S. Air Force.

[18] Peng, T. and Pindroh, A. L., "An Improved Calculation of Gas Properties at High Temperatures-Air," *Magnetohydrodynamics*, 4th Biennial Gas Dynamics Symposium, American Rocket Society and Northwestern Univ., edited by Cambel, A. B., Anderson, T. P., and Slawsky, M. M., Northwestern Univ. Press, 1961, pp. 67–88.

[19] Hansen, F. C., "Approximations for the Thermodynamic and Transport Properties of High Temperature Air," TR R-50, 1959, NASA.